Contribution from the Departments of Chemistry, Sonoma State University, Rohnert Park, California 94928, and University of Washington, Seattle, Washington 98195

The Vapor Phase Formed by Reaction of Mixtures of Aluminum, Gold, and Chlorine

D. S. Rustad† and N. W. Gregory*,‡

Received October 23, 1991

A spectrophotometric study of mixed-metal dimers in vapors formed by reaction of Al, Au, and Cl_2 is presented. The absorbance of fully vaporized mixtures as well as the gas phase in equilibrium with Au(s) has been observed at various concentrations of Al_2Cl_6 and Cl_2. While $AlAuCl_6(g)$ appears to be the dominant mixed-metal dimer, evidence is found suggesting the presence of molecules containing less chlorine, such as $AlAuCl_5(g)$. Assuming both $AlAuCl_6(g)$ and $AlAuCl_5(g)$ are present, thermodynamic properties and UV-visible absorption spectra are derived.

We report a UV-visible spectrophotometric study of vapors formed by reactions of mixtures of aluminum, gold, and chlorine, including all vapor systems as well as vapors in equilibrium with metallic gold. In the heterogeneous systems the amount of gold in the vapor phase, at a given chlorine pressure, is greatly enhanced by the presence of aluminum chloride. This is attributed to the formation of mixed-metal-dimer molecules. The variation of the absorbance with chlorine and aluminum chloride partial pressures indicates that $AlAuCl_6$ is the dominant mixed-metal-dimer species, with the possible presence of $AlAuCl_5$ and/or $AlAuCl_4$.

The absorption spectrum of the mixed-metal-dimer vapor is compared with that recently reported for $Au_2Cl_6(g)$.[1] Molar absorptivities at 10-nm intervals in the range 200-600 nm and thermodynamic properties are derived. This study follows earlier work from this laboratory on the similar molecules $AlFeCl_6$[2] and $AlFeBr_6$.[3]

Experimental Section

Samples. Seven different mixtures (Table I) in quartz cells were equilibrated in the range 440-725 K. Temperatures were measured with chromel-alumel thermocouples, calibrated at the melting point of tin. Vapor-phase absorbances between 200 and 600 nm were measured with a Cary 14H spectrophotometer. The quartz absorption cells and furnace assembly have been described previously.[4] The samples of gold (Morgan Hastings Co., "Pure" gold),[1] aluminum (wire, 0.032 in., Baker analyzer reagent, 99.9%), and silicon[5] were weighed with a Cahn 21 automatic electrobalance. For each sample the cell, containing the solid elements, was connected to the vacuum system by a quartz side arm. Chlorine, generated by heating copper(II) chloride (Baker Adamson reagent), was condensed in another side arm with liquid nitrogen. The condensed chlorine was allowed to warm until the desired amount of chlorine gas, determined by observing the chlorine absorbance at 330 nm (peak maximum), had entered the cell. The side arm was then sealed off. An excess of chlorine, over the amount needed to react with the solid elements, was added to prevent decomposition of gold(III) chloride at lower temperatures. The amounts of chlorine listed in Table I are values which minimize the deviations between calculated and observed absorbances for all observations made for each sample at 330 nm. A successive approximation procedure was used to correct for the small absorbance contribution made by the gold halide vapors at this wavelength (see following discussion). The temperature dependence of the molar absorptivity of chlorine at 330 nm, $\epsilon_c = 82.0 - 0.0529T + 1.427 \times 10^{-5}T^2$ L mol^{-1} cm^{-1}, was taken from earlier work.[1,6]

To obtain the very small samples of aluminum, the source wire was hammered into a thin film. Small sections were removed with a razor blade and weighed. After the absorbance measurements, the amounts of aluminum in samples 4-7, and silicon in sample 7, were also determined by analyses of 1% nitric acid solutions of the cell contents, using an ICP atomic emission spectrometer (Model 955, Plasmo Atomcorp). Aluminum standards were prepared from the aluminum wire and silicon standards by dilution of a 1000-ppm standard solution (Baker Instra-Analyzed atomic spectra) with 1% nitric acid solution. Amounts of aluminum found by analysis (listed in Table I) averaged 96.4% of the sample masses weighed on the balance. After reaction of the aluminum with chlorine, a small amount of oxide residue could be seen in the cell. An aluminum analysis had not been made on samples 1-3; since all samples were taken from the same piece of hammered wire, it was assumed for samples 1-3 that the actual masses of aluminum (listed in Table I) were 96.4% of the weighed sample masses.

Table I. Cell Path Lengths, Volumes, and Initial Amounts of Reactants

sample no.	Pl, cm[a]	V, cm^3 [b]	μmol of Au[c]	μmol of Al[d]	μmol of Cl_2[d]	μmol of Cl_2[e]
1	10	30.89	0.310	28.5	70.0	26.6
2	5	15.41	0.350	8.25	66.9	54.0
3	1	3.653	0.352	7.40	69.6	57.9
4	10	29.78	0.262	21.5	55.5	22.9
5	10	29.26	0.262	21.1	41.3	9.32
6	1	3.796	0.221	8.03	35.0	22.6
7[f]	1	3.890	0.269	8.52	77.1	42.9

[a] Path length ±0.001, certified by Pyrocell Mfg. Co., Westwood, NJ. [b] Determined from mass of water necessary to fill cell. [c] Estimated uncertainties ±0.003. [d] Estimated uncertainties ±1-2%. [e] Cl_2 remaining after Al and Au converted to their trichlorides. [f] 10.5 μmol of Si included to form $SiCl_4$.

The amounts of the elements and the temperature ranges of the study were selected so that the metal chlorides were all in the vapor phase. At the highest temperatures, vapors were in equilibrium with a solid phase. A separate experiment was carried out to generate a sufficient amount of the solid to determine its crystal structure. A 1-cm cell (4.42-mL volume) containing 13.0 μmol of gold, 27.6 μmol of aluminum, and 120 μmol of chlorine was held at 460 K for 2 days to convert the metals to their chlorides. The cell side arm and cell body were then held at 590 and 540 K, respectively, for 15 h. Crystals with a metallic appearance, resembling gold, were formed in the side arm. The cell body was immersed in liquid nitrogen and the side arm held at 420 K for about 1 min to remove volatile chlorides. In a drybox, the metallic crystals were transfered to and sealed in capillary tubes. X-ray examination of a single crystal as well as a crystalline aggregate indicated that both were gold (face-centered cubic cell, $a_0 = 0.407$ nm).[7]

Interaction of $Al_2Cl_6(g)$ with Quartz. The interaction of $Al_2Cl_6(g)$ with quartz[8] was examined in several experiments. A mixture of Al and 48.8 μmol of Cl_2 was held in a quartz cell, volume 3.843 mL, for 193 h at 693 K. The vapor was condensed in the cell with liquid nitrogen and 1% HNO_3 solution added to dissolve the contents. Amounts of Si, 0.676 μmol, and Al, 9.51 μmol, were determined by analysis (ICP). The concentration ratio $SiCl_4/Al_2Cl_6$ was found to be 0.17, in excellent agreement with that predicted from thermodynamic data[9] if the reaction $Al_2Cl_6(g) + SiO_2(s) = 2\ AlOCl(s) + SiCl_4(g)$ establishes equilibrium. AlOCl(s) is soluble in acidic solution. Only sample 7 was studied at temperatures this high, maximum equilibration periods 24 h, and here silicon was included (see Table I) to generate a concentration of $SiCl_4(g)$

* Author to whom correspondence should be addressed.
† Sonoma State University.
‡ Univeristy of Washington.

(1) Rustad, D. S.; Gregory, N. W. *Polyhedron* **1991**, *10*, 633.
(2) Shieh, C.-F.; Gregory, N. W. *J. Phys. Chem.* **1975**, *9*, 828.
(3) Gregory, N. W.; Laughlin, W. C. *J. Phys. Chem.* **1977**, *81*, 2228.
(4) Rustad, D. S.; Gregory, N. W. *Inorg. Chem.* **1988**, *27*, 2840.
(5) Crystals of silicon were provided by Professor D. M. Ritter.
(6) Seery, D. J.; Britton, D. *J. Phys. Chem.* **1964**, *68*, 2266. Burns, G.; Norrish, R. G. W. *Proc. R. Soc. (Lond), Ser A* **1963**, *271*, 289. Gibson, G. E.; Bayliss, N. S. *Phys. Rev.* **1933**, *44*, 188.
(7) We thank Dr. S. C. Critchlow for the X-ray analysis.
(8) Schäfer, H.; et al. *Z. Anorg. Allg. Chem.* **1950**, *263*; 87; **1958**, *297*, 48; **1977**, *433*, 58; **1978**, *448*, 129.
(9) Chase, M. W., Jr.; Davies, C. A.; Downey, J. R.; Frurip, D. J.; McDonald, R. A.; Syverud, A. N. *JANAF Thermochemical Tables*, 3rd ed.; American Chemical Society and American Institute of Physics: New York, 1986.

0020-1669/92/1331-1774$03.00/0

large enough to prevent formation of AlOCl(s).

In a similar experiment 8.60 μmol of Al and 41.6 μmol of Cl_2 in a cell with volume 3.775 mL was held at 664 K for 52 h. The amount of silicon in the vapor in this case (0.473 μmol) was only half the value expected for equilibrium with AlOCl(s). This temperature is in the upper range in which samples 3 and 6 were studied, and for these the longest equilibration period was 24 h. As discussed below, results from samples 3, 6, and 7 are in good agreement when the interaction with quartz is neglected.

In two additional experiments, 26.4 μmol of Al, 44.3 μmol of Cl_2, and 0.320 μmol of Au in a cell with volume 31.03 mL and 22.2 μmol of Al, 59.8 μmol of Cl_2, and 0.461 μmol of Au in a cell with volume 30.11 mL, the amounts of silicon found in vapors held at 581 K for 24 h were very small ($SiCl_4/Al_2Cl_6$ ratios less than 0.01; equilibrium value 2.5). The maximum temperatures used for samples 1, 4, and 5 were 578, 576, and 529 K, respectively, and equilibration times were no longer than 24 h.

Results and Discussion

Vapors generated by the Al–Au–Cl_2 mixtures give an absorption spectrum generally similar to that of $Au_2Cl_6(g)$, with a strong absorption band (charge-transfer transition) in the ultraviolet and a weaker band (d–d transition) around 460 nm. However only a single maximum, ca. 230 nm, is observed in the ultraviolet, whereas Au_2Cl_6 has two peaks, ca. 220 and 240 nm.[1] At comparable chlorine concentrations and with vapors in equilibrium with Au(s), all mixtures gave absorbances much higher, by factors ranging from 15 to several hundred, than those observed for gold–chlorine mixtures. Because $Al_2Cl_6(g)$ does not absorb light appreciably at wavelengths greater than 210 nm, it was assumed that these differences indicate the presence of mixed-metal-dimer molecules.

Under our equilibrium conditions, $Al_2Cl_6(g)$ dissociates only slightly and $Au_2Cl_6(g)$ not measurably into their respective monomers.[1,9] The dimers may be expected to equilibrate, reaction 1, to form a mixed-metal dimer. On statistical grounds this

$$Al_2Cl_6(g) + Au_2Cl_6(g) = 2AlAuCl_6(g) \quad (1)$$

reaction should have an equilibrium constant around unity. The number of moles of aluminum in the various samples (see Table I) is substantially greater than the number of moles of gold. Hence, when the samples are fully vaporized, virtually all the gold should be in mixed-metal-dimer molecules.

Above a certain temperature, depending on the composition of the mixture, vapor absorbances were observed to decrease as the temperature was increased. A similar behavior, associated with equilibrium 2, was observed in the Au–Cl_2 system. A similar

$$2Au(s) + 3Cl_2(g) = Au_2Cl_6(g) \quad (2)$$

equilibrium, (3), is believed responsible in the Al–Au–Cl_2 system.

$$Au(s) + 0.5Al_2Cl_6(g) + 1.5Cl_2(g) = AlAuCl_6(g) \quad (3)$$

With the samples equilibrated at high temperatures, the clam-shell furnace was opened and the cells inspected. Tiny gold crystals (see Experimental Section) were observed on the wall of the side arm at the location closest to the external heating element for the cell body. The temperature, T_s, at this point was several degrees above that of the main cell body, T_g. If reaction 3 is exothermic, as is reaction 2, gold would be expected to deposit on the surface at the highest temperature.

To test the assumption that the composition of the vapor in equilibrium with Au(s) is controlled by reactions 2 and 3, the relationship between the absorbance at the peak maximum, 230 nm, and the chlorine and aluminum chloride concentrations in the various samples was examined. Under the conditions of the present study, $Al_2Cl_6(g)$ is expected, on thermodynamic grounds, to react with quartz, forming $SiCl_4(g)$ and AlOCl(s) or, as the more stable product, $Al_2O_3(s)$.[8] These reactions are kinetically inhibited, however. On the basis of the observations described in the Experimental Section, we have assumed that the interaction with quartz has not affected the concentration of Al_2Cl_6 outside the range of other experimental uncertainties.

Derivation of Equilibrium Constants and Concentrations. If $AlAuCl_6(g)$ is the only mixed-metal dimer present, the following equilibrium concentration relationships may be written: $C_c = C_0(Cl_2) - 1.5C_0(Al) - 1.5C_6 - 3C_{Aud}$, where C_c is the free chlorine concentration, $C_0(Cl_2)$ and $C_0(Al)$, respectively, are the concentration equivalents of the number of moles of chlorine and aluminum introduced, C_6 is the concentration of $AlAuCl_6(g)$, and C_{Aud} is the concentration of $Au_2Cl_6(g)$. $C_{Ald} = 0.5(C_0(Al) - C_m - C_6)$, where C_{Ald} and C_m, respectively, are the concentrations of $Al_2Cl_6(g)$ and $AlCl_3(g)$. C_{Ald} and C_m are related by the equilibrium constant for the reaction $Al_2Cl_6(g) = 2AlCl_3(g)$, where $K_{Ald} = C_m^2RT/C_{Ald}$. Values of K_{Ald} were derived from data in the JANAF tables.[9] With Au(s) present, values of C_{Aud} were derived from the equation $C_{Aud} = K_2C_c^3(RT)^2$, with $\ln K_2 = 12959/T_s - 29.011$.[1]

The various concentrations were derived from the absorbance data by successive approximations. It was assumed that the total absorbance $A_t = A_{obs}/Pl$, where Pl is the path length, is given by Beer's law: $A_t = \epsilon_6C_6 + \epsilon_cC_c + \epsilon_{Aud}C_{Aud}$; the respective ϵ values are the appropriate molar absorptivities. An initial trial value of the molar absorptivity of $AlAuCl_6(g)$ at 230 nm was assigned as follows. Because ϵ_c is virtually zero at 230 nm and the ratio C_{Ald}/C_{Aud} is very large, the absorbance is mainly due to $AlAuCl_6(g)$; hence when all the gold is in the vapor phase, ϵ_6 may be approximated as $A_{230}/C_0(Au)$. To allow for the variation of ϵ_6 with temperature, a least-squares treatment of values from all samples (29 observations; see Table S1, supplementary material) was used to derive the constants a and b in an empirical equation of the form $\epsilon_6 = a + bT$. Initially, the relationship $C_{Al} = C_0(Al) = C_m + 2C_{Ald} = C_m + 2RTC_m^2/K_{Ald}$ was used to derive values of C_{Ald}, since C_6 is small compared to C_{Al}. *Now with Au(s) present*, an initial trial value of C_c as $C_0(Cl_2) - 1.5C_0(Al)$ was used with K_2 to find C_{Aud}. A_6, the absorbance of $AlAuCl_6(g)$, was then taken as $A_t - A_{Aud}$, where A_{Aud} is the absorbance of $Au_2Cl_6(g)$, $24790C_{Aud}$ at 230 nm,[1] and C_6 was A_6/ϵ_6. Values of C_{Al} were then corrected to $C_0(Al) - C_6$ and C_c to $C_0(Cl_2) - 1.5C_0(Al) - 1.5C_6 - 3C_{Aud}$. The calculation was repeated until further cycling led to no changes in the concentrations. Finally, values of K_1, $K_1 = C_6^2/C_{Ald}C_{Aud}$, and a least-squares equation of the form $\ln K_1 = B/T_g + A$, were derived for use with all vapor mixtures.

The equation initially derived for ϵ_6 was then refined by reprocessing the data with *all the gold in the vapor phase*. In this case C_{Aud} is not fixed by equilibrium 2. The relationships $C_0(Al) - C_0(Au) = C_m + 2C_{Ald} = C_m + 2C_m^2RT/K_{Ald}$, which neglects the relatively small C_{Aud}, and $C_0(Au) = C_6 + 2C_{Aud} = C_6 + 2C_6^2/C_{Ald}K_1$ were used to derive concentrations in the all vapor mixtures. A_6 now equals $A_{230} - 24790C_{Aud}$, which led to a corrected equation for ϵ_6. The new approximation for ϵ_6 was then used in a repeat of the treatment of the data with Au(s) present. No significant changes occurred after three or four cycles. At 230 nm A_{Aud} was generally small, less than 1% of A_t for samples 1, 4 and 5 and somewhat larger, maximum 9%, for the others.

The "absorbance constant" for equilibrium 3, $K_{3a}(I) = A_6/C_cRT(C_cC_{Ald})^{0.5}$, was derived for each of the 45 observations (see Table S1, supplementary material). In this and in equations to follow, the subscript "a" is used to denote use of absorbances in place of concentrations, and "(I)" indicates only one mixed-metal dimer assumed present. A least-squares treatment of $\ln K_{3a}(I)$ vs $1/T_s$ gave the result

$$\ln K_{3a}(I) = 6463.2\ (\pm 1.2\%)/T_s - 4.352\ (\pm 3.0\%)$$

Relative standard deviations are shown in parentheses. The various samples show a good general correlation; see the scatter of points in Figure 1. However, the standard deviations of the constants are somewhat larger than expected from the uncertainties in the absorbances. Furthermore it is observed that the various samples, when grouped by similar chlorine concentrations (see caption for Figure 1), generate a series of approximately parallel lines; least-squares lines are shown in Figure 1. Lines for samples with lower chlorine concentrations are above those for samples with higher chlorine concentrations.

These systematic shifts can be largely eliminated if it is assumed that another light-absorbing molecule, in addition to $AlAuCl_6$ and Au_2Cl_6, is present. This is conveniently illustrated by comparing

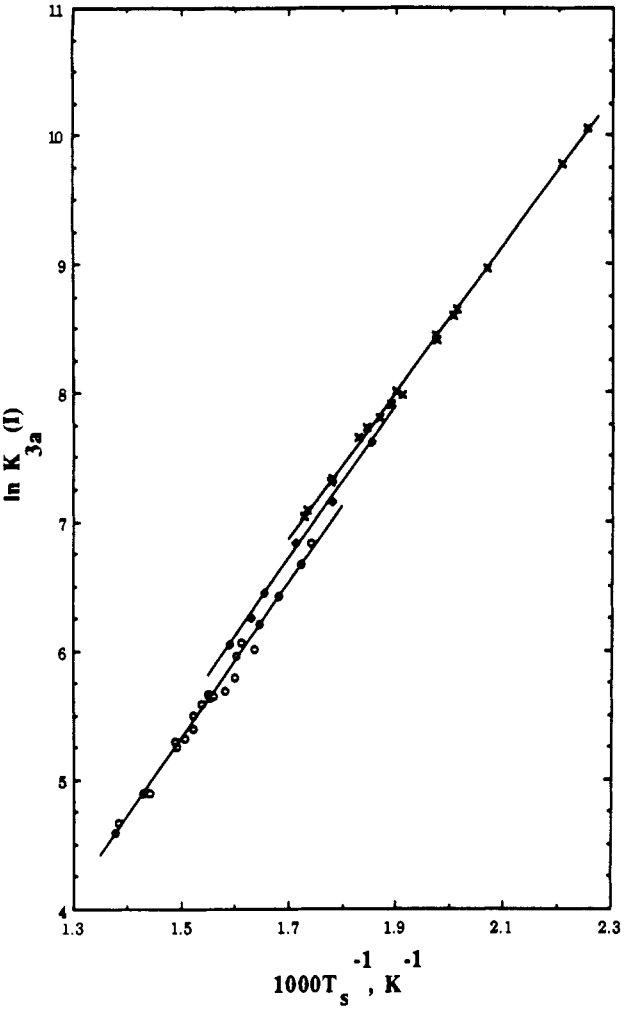

Figure 1. ln K_{3a}(I) vs $1/T_s$. Least-squares lines shown for the samples are grouped by symbols: ×, samples 1, 4, and 5; ◆, sample 2; ○, samples 3, 6, and 7.

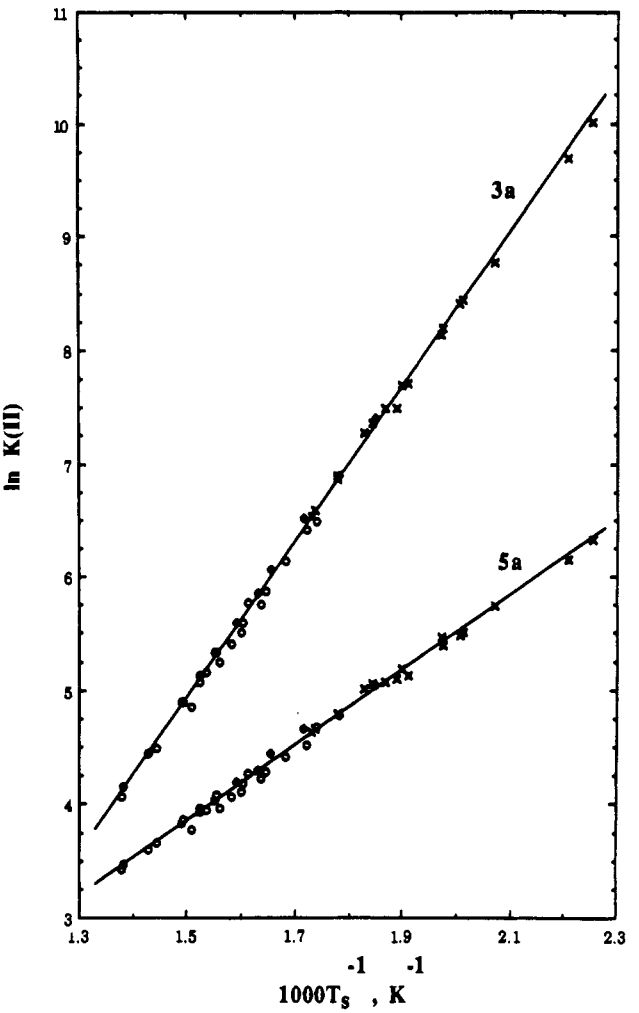

Figure 2. ln K(II) vs $1/T_s$. Symbols are identified in the Figure 1 caption. Least-squares lines are shown for equilibrium 3, K_{3a}(II), and equilibrium 5, K_{5a}, respectively.

absorbances observed at T_s ca. 575 K for samples 4 and 6, which have significantly different chlorine concentrations. If an equilibrium of the general form

$$x\mathrm{Au(s)} + (y/2)\mathrm{Al_2Cl_6(g)} + ((z-3y)/2)\mathrm{Cl_2(g)} = \mathrm{Al}_y\mathrm{Au}_x\mathrm{Cl}_z\mathrm{(g)} \quad (4)$$

is considered along with reactions 2 and 3, one then has $A_t - A_{Aud} = A_6 + A_z = K_{3a}(II)C_cRT(C_{Ald}C_c)^{0.5} + K_4f(c)$. K_4 is the equilibrium constant for reaction 4 and the form of $f(c)$ is fixed by the coefficients in the selected reaction. From two independent equations, one from sample 4 and one from sample 6, the required values of K_{3a}(II) and K_4 may be obtained. (The value of x cannot be fixed from absorbance data; for simplicity it is assumed to be 1.) Of all possibilities for y, only $AlAuCl_4$, $AlAuCl_5$, Al_2AuCl_7, Al_2AuCl_8, Al_3AuCl_{10}, and Al_4AuCl_{13} give positive K_4 values. If each of these molecules is used in a successive approximation procedure, only the first two give accompanying values of K_{3a}(II), which, on least-squares treatment, give results with standard deviations appreciably less than that when only reactions 2 and 3 are used. The result if $AlAuCl_5$(g), reaction 5, is selected will be illustrated.

$$\mathrm{Au(s)} + 0.5\mathrm{Al_2Cl_6(g)} + \mathrm{Cl_2(g)} = \mathrm{AlAuCl_5(g)} \quad (5)$$

The concentration relationships are now $C_c = C_0(Cl_2) - 1.5C_0(Al) - 1.5C_6 - C_5 - 3C_{Aud}$ and $C_{Ald} = 0.5(C_0(Al) - C_m - C_6 - C_5)$, where C_5 represents the concentration of $AlAuCl_5$. As before, in the first approximations for C_c and C_{Ald}, C_5 and C_6 were initially ignored; their effects were finally included by successive approximations. The pertinent absorbance equation, with A_5 as the contribution of $AlAuCl_5$, is now $A_t - A_{Aud} = A_5 + A_6 = K_{5a}C_c(C_{Ald}RT)^{0.5} + K_{3a}(II)C_cRT(C_cC_{Ald})^{0.5}$. From the equations given by samples 4 and 6, the required values of K_{5a} and K_{3a}(II) at 575 K were derived. To obtain values at other temperatures, it was found convenient to use equilibrium constants for the related vapor-phase reaction 6, where $K_{6a} = K_{5a}/K_{3a}(II)$. Now

$$\mathrm{AlAuCl_6(g)} = \mathrm{AlAuCl_5(g)} + 0.5\mathrm{Cl_2(g)} \quad (6)$$

$= A_5 + A_6 = A_6(1.0 + (K_{6a}/(C_cRT)^{0.5}))$. Assuming ln $K_{6a} = \beta_6/T_g + \alpha_6$, the constants α_6 and β_6 must be related by the value of K_{6a} at 575 K. Trial values of one constant, e.g. β_6, then lead to values of A_5 and A_6 for each sample at the temperature at which the absorbance was measured. Using absorbances at 230 nm for all samples, values of β_6 were varied so as to reduce the standard deviations in the least-squares result for K_{3a}(II). The best result was obtained using ln $K_{6a} = -3630/T_g + 4.481$, which gave the least-squares equations

$$\ln K_{3a}(II) = 6824.0\ (\pm 0.64\%)/T_s - 5.305\ (\pm 1.4\%)$$

$$\ln K_{5a} = 3298.5\ (\pm 1.1\%)/T_s - 1.099\ (\pm 5.4\%)$$

The constants in these equations give, for reaction 6, ln $K_{6a} = -3525/T_g + 4.206$, a result which differs from the assumed equation by slightly more than the variation expected from the standard deviations. This difference persists when the calculation is repeated using the modified expression for ln K_{6a}. The constants showed no tendency to converge after several successive approximations, and the standard deviations for ln K_{3a}(II) and ln K_{5a} began to increase. Hence, we have used the result as derived above.

The ln K vs $1/T$ plots, along with the least-squares lines, are shown in Figure 2. The scatter of points is well within experi-

Table II. Molar Absorptivities Assigned to $AlAuCl_6(g)$, Assumed as the Only Mixed-Metal Dimer (435–707 K)

wl, nm	$10^{-3}a_\lambda$	b_λ	wl, nm	$10^{-3}a_\lambda$	b_λ	wl, nm	ϵ_λ	wl, nm	ϵ_λ
200	−3.14	12.4	310	−1.97	5.65	420	428	520	380
210	5.75	4.37	320	−1.96	5.12	430	562	530	310
220	16.65	−5.03	330	−1.67	4.10	440	640	540	220
230	19.81	−6.38	340	−2.18	4.92	450	660	550	150
240	15.07	−0.20	350	−1.82	4.18	460	750	560	80
250	7.72	6.88	360	−1.35	3.04	470	770	570	50
260	1.90	10.7	370	−1.04	2.50	480	720	580	50
270	−0.57	10.1	380	−0.58	1.61	490	670	590	40
280	−0.88	7.63	390	−0.75	1.94	500	560	600	30
290	−1.13	6.29	400	−0.76	1.95	510	500		
300	−2.09	6.77	410	−0.37	1.37				

mental uncertainty. The shifts correlating with chlorine concentrations, seen in Figure 1, are no longer apparent, and the standard deviations of the enthalpy and entropy constants are now significantly less. Values of K_{1a}, $A_6^2/C_{Ald}A_{Aud}$, were calculated from the derived absorbances, and from these come a least-squares equation of the form $\ln K_{1a} = B/T_g + A$ for use in the treatment of the all-vapor mixtures.

To derive concentrations in the *completely vaporized mixtures*, K_{1a} and K_{6a} were used to calculate A_6, A_5, and A_{Aud} (at 230 nm). $A_t = A_5 + A_6 + A_{Aud} = A_6(1.0 + (K_{6a}/(C_cRT)^{0.5})) + A_6^2/C_{Ald}K_{1a}$. In the initial approximation C_{Ald} values were obtained from $C_0(Al) - C_0(Au) = C_m + 2C_{Ald}$ and K_{Ald}, which neglects the small correction for C_{Aud}. C_c was taken as $C_0(Cl_2) - 1.5(C_0(Al) + C_0(Au))$, which neglects a small correction for the lesser amount of chlorine in $AlAuCl_5$. The initial approximation for C_{Aud} was then given by $A_{Aud}/24790$.[1] Now, $C_0(Au) - 2C_{Aud} = C_5 + C_6$ and $C_5 = A_5/\epsilon_5$ and $C_6 = A_6\epsilon_6$. To derive trial values of ϵ_6 and ϵ_5, a least-squares treatment of $A_6/(C_0(Au) - 2C_{Aud}) = a_6 + b_6T - (\epsilon_6/\epsilon_5)(A_5/C_0(Au) - 2C_{Aud})$, which assumes $\epsilon_6 = a_6 + b_6T$ and treats ϵ_6/ϵ_5 as a constant. Values of C_6 and C_5 were then derived, $C_i = A_i/\epsilon_i$. These concentrations were then used in least-squares treatments of $A_t - A_{Aud} = (a_5 + b_5T)C_5 + (a_6 + b_6T)C_6$ to derive "improved" molar absorptivities. C_6, C_5, and C_{Aud} were then used to derive new values of C_c and C_{Ald}, and the whole treatment was repeated until consistent values were obtained.

Temperatures, observed absorbances at 230 and 330 nm, and the derived concentrations are listed in Table S1 (supplementary material). Only T_g is given for the all-vapor mixtures. $AlAuCl_6(g)$ appears to be the dominant mixed-metal dimer in the all-vapor mixtures, which have C_5/C_6 ratios between 0.07 and 0.33; ratios tend to be higher (between 0.31 and 0.98) in vapors in equilibrium with Au(s), which are, for the most part, at higher temperatures.

A similar improvement of fit is obtained if $AlAuCl_4(g)$ is assumed present instead of $AlAuCl_5(g)$; the absorbance data do not distinguish between the two possibilities. In view of the relatively low volatility of AuCl(s), it seems less likely that $AlAuCl_4(g)$ makes a significant contribution. Also, Au(I) compounds are not expected to have a significant ligand–metal charge-transfer absorption spectrum in the wavelength range studied. As the oxidation number of the gold atom decreases, its electronegativity also decreases, resulting in an expected shift of the charge-transfer transition to higher energies. From trends in optical electronegativites,[10,11] an Au(I)–Cl charge-transfer transition would be expected to occur at an energy about twice that for Au(III)–Cl, with the energy for Au(II)–Cl in between.

Although Au(II) compounds in the condensed state are not known,[12] the evidence seen here suggests that gold(II) chloride and aluminum(III) chloride may form a reasonably stable mixed-metal dimer in the vapor phase. Possibly the two metal atoms share three chlorine atoms, i.e. share the face of two distorted tetrahedra, with an additional chlorine atom attached to each, or the metal atoms may be bridged by sharing two chlorine atoms, with one additional chlorine atom bonded to Au(II) and two to Al(III). Both structures have been proposed for other mixed-metal-dimer molecules of the general form MLX_5.[13] In addition, Au(I) has a $5d^{10}$ electronic configuration which requires the charge-transfer electron to go into a higher energy 6s orbital.

Even though the absorbance data can be reasonably explained using a combination of two mixed-metal dimers, the possibility that the vapor is a more complex mixture cannot be ruled out.

Molar Absorptivities If $AlAuCl_6$ Is the Only Mixed-Metal Dimer Present. Molar absorptivities for $AlAuCl_6(g)$, $\epsilon_{6,\lambda}$, were calculated at 10-nm intervals over the range 200–600 nm using the values of C_6 derived from the absorbance at the peak maximum, 230 nm, when $AlAuCl_6$ was assumed the only mixed-metal dimer. In general $A_{6,\lambda} = A_\lambda - A_{c,\lambda} - A_{Aud,\lambda}$; i.e., the contributions of chlorine, A_c, and of Au_2Cl_6, A_{Aud}, must be subtracted from the total absorbance. At wavelengths below 420 nm, a least-squares treatment based on empirical equations of the form $\epsilon_\lambda = a_\lambda + b_\lambda T_g$ was used to allow for the variation of $\epsilon_{6,\lambda}$ with temperature. At longer wavelengths an average value was derived. Results are shown in Table II.

Values of D_{abs}, the absolute value of $A_{obs} - Pl(\epsilon_cC_c + \epsilon_{Aud}C_{Aud} + \epsilon_6C_6)$, for each observed absorbance, A_{obs}, 1599 observations, were examined as a test of fit. Of these, 390 lie in the range 200–290 nm, where the contribution of the molecules containing gold is large. The change of absorbance with wavelength in this interval is very large leading to a rather large estimated uncertainty for A_{obs}, 0.022, associated with fixing the wavelength, the measurement of A_{obs}, the baseline, and the temperature. A rather large number, 62, of values of D_{abs} exceeded this estimate (none in the range 300–600 nm). As shown in following paragraphs, the fit is improved significantly if $AlAuCl_5(g)$ is also assumed present.

Molar Absorptivities If Both $AlAuCl_6$ and $AlAuCl_5$ Are Assumed Present. The concentrations derived when both $AlAuCl_5$ and $AlAuCl_6$ were assumed present (Table S1) were used in least-squares treatments of $A_t - A_{Aud} - A_c = C_5(a_{\lambda5} + b_{\lambda5}T_g) + C_6(a_{\lambda6} + b_{\lambda6}T_g)$, at 10-nm intervals over the range 200–310 nm, to derive equations of the form $\epsilon_\lambda = a_\lambda + b_\lambda T_g$ for $\epsilon_{\lambda5}$ and $\epsilon_{\lambda6}$. In the range 320–410, $\epsilon_{6,\lambda}$ was treated as a constant and $\epsilon_{5,\lambda}$ as a temperature-dependent function. At longer wavelengths, both molar absorptivities were treated as constants. The least-square values were adjusted slightly when this was found to reduce the number of D_{abs} values exceeding 0.022. Results are shown in Table III. Now only 32 values of D_{abs}, the absolute value of $A_{obs} - Pl(C_c\epsilon_c + C_{Aud}\epsilon_{Aud} + C_5\epsilon_5 + C_6\epsilon_6)$, exceed 0.022, half the number when $AlAuCl_5$ was excluded. Of these, only 12 were found at wavelengths above 220 nm. The remainder, at 200, 210, and 220 nm, are near the short wavelength limit of the instrument where experimental uncertainties are appreciably larger. Derived absorption spectra for $AlAuCl_6(g)$ and $AlAuCl_5(g)$ are shown in Figure 3 at 550 K, the mean temperature for the all-vapor observations.

General Discussion of Spectra. The specific geometries of the gas-phase dimers are unknown, and thus, only a general discussion of the spectra can be given. The local geometry of the chlorine

(10) Jorgensen, C. K. *Orbitals in Atoms and Molecules*; Academic Press: New York, 1962; p 96.
(11) Lever, A. B. P. *Inorganic Electronic Spectroscopy*, 2nd ed.; Elsevier: New York, 1984.
(12) James, S. E.; Hager, J. P. *Metall. Trans.* **1978**, *9B*, 501. Hager, J. P.; Hill, R. B. *Ibid.* **1970**, *1*, 2723.
(13) Papatheodorou, G. N. *Current Topics in Materials Science*; Kaldis, E., Ed.; North-Holland: Amsterdam, 1982; p 250.

Table III. Molar Absorptivities, $\epsilon_{5,\lambda}$ and $\epsilon_{6,\lambda}$, Assigned to $AlAuCl_5(g)$ and $AlAuCl_6(g)$, Assumed as the Only Mixed-Metal Dimers Present (435–707 K)

wl, nm	$10^{-3}a_6$	b_6	$10^{-3}a_5$	b_5	wl, nm	ϵ_6	$10^{-3}a_5$	b_5	wl, nm	ϵ_6	ϵ_5
200	−0.83	9.90	−6.81	12.5	340	50	0.89	1.32	480	740	540
210	7.96	0.24	0.15	12.8	350	30	0.91	0.72	490	680	540
220	20.87	−13.8	15.02	−13.9	360	20	−0.47	2.49	500	590	450
230	21.16	−7.73	16.38	−5.86	370	20	0.42	1.16	510	510	420
240	13.69	3.67	14.94	−6.60	380	20	1.76	−1.46	520	400	280
250	6.18	10.8	7.84	1.20	390	55	0.36	1.06	530	280	220
260	0.37	14.1	5.94	0.49	400	90	0.38	1.01	540	200	160
270	−0.41	9.78	1.71	5.20	410	150	2.84	−3.15	550	155	120
280	0.08	5.40	1.60	3.97	420	280	0.80		560	100	80
290	1.23	0.93	0.68	5.51	430	480	0.68		570	60	50
300	2.79	−3.47	−6.14	17.1	440	640	0.54		580	50	30
310	2.97	−4.51	−6.89	16.9	450	710	0.38		590	40	20
320	0.18		6.60	−6.67	460	780	0.46		600	30	10
330	0.07		4.96	−5.28	470	780	0.46				

Table IV. Thermodynamic Constants[a,b] at Mean Temperature 600 K ($\ln K = BT^{-1} + A$)

					$AlAuCl_6(g)$		$AlAuCl_5(g)$	
reacn[c]	B	A	$\Delta H°$	$\Delta S°$	$\Delta H°_f$	$S°$	$\Delta H°_f$	$S°$
1 (I)	−208 (±73%)	1.20 (±22%)	1.73	10.0	−698	624		
1 (II)	429 (±20%)	−0.60 (±25%)	−3.57	−5.0	−704	609		
3 (I)	6348 (±1.2%)	−13.84 (±0.94%)	−52.78	−115.1	−699	619		
3 (II)	6681 (±0.63%)	−14.78 (±0.49%)	−55.54	−122.9	−702	611		
5 (II)	3164 (±1.1%)	−10.34 (±0.57%)	−26.30	−85.9			−673	524

[a] Reference data; Al_2Cl_6,[9] Cl_2,[9] Au_2Cl_6,[1] and Au.[20] [b] $\Delta H°$, kJ mol^{-1}; $S°$, J K^{-1} mol^{-1}. [c] (I) Assuming $AlAuCl_6(g)$ is the only mixed-metal dimer; (II) assuming both $AlAuCl_6(g)$ and $AlAuCl_5(g)$ are present.

atoms about the gold atom in $AlAuCl_6(g)$ is probably distorted square planar due to having terminal and bridging chlorine atoms. The $[AuCl_4]^-$ ion is square planar, D_{4h},[14] and solid gold(III) chloride contains slightly distorted square-planar dimeric Au_2Cl_6 molecular units.[15] The local geometry about the gold atom in $AlAuCl_5(g)$ is probably distorted trigonal planar or tetrahedral as discussed earlier.

Spectra of $AlAuCl_6(g)$ (Figure 3), $AlAuCl_5(g)$ (Figure 3), $Au_2Cl_6(g)$,[1] $Au_2Cl_6(s)$,[16] and the $[AuCl_4]^-$ ion[14] show similarities in transitional energies but differences in molar absorptivities. The spectrum of $Au_2Cl_6(g)$ shows distinct peaks at the following wavelengths in nm (molar absorptivities per Au atom in cm^{-1} mol^{-1} L at 550 K): 222 (12 550), 244 (15 400), and 460 (970). Solid gold(III) chloride film gives distinct peaks at 293 K of 230, 320, 358, and 438 nm and at 83 K of 230, 320, and 438 nm. The spectrum for the $[AuCl_4]^-$ ion has been studied by several workers at 300 and 77 K, with different cations and in various solvents. The following are representative transitional wavelengths, molar absorptivities, and assignments: 226 (44 250; LMCT, $^1E_u(2) \leftarrow {}^1A_{1g}$), 322–329 (5020–6500; LMCT, $^1A_{2u}, {}^1E_u(1) \leftarrow {}^1A_{1g}$), 400–380 (304–267; $^1E_g \leftarrow {}^1A_{1g}$), and 460 (15; $^1A_{2g} \leftarrow {}^1A_{1g}$). The energy order of the d-orbitals in the square-planar field is $b_{1g}(x^2 - y^2) > b_{2g}(xy) > e_g(xz,yz) > a_{1g}(z^2)$. All of these species show the d–d transition at about 460 nm but with quite different molar absorptivities. The dimers have much higher values per gold atom than the ion. Even though molar absorptivities for the peaks in the solid spectra are not attainable, the 358- and 438-nm peaks are definitely enhanced relative to the 230- and 320-nm peaks. This difference in molar absorptivities could be due to the asymmetry of terminal and bridging chlorine atoms in the dimers compared to the symmetrical D_{4h} ion. Also, this transition involves transferring an electron from a π-antibonding orbital (b_{2g}) to a σ-antibonding orbital (b_{1g}) causing vibronic coupling. Both of these effects cause relaxation of the Laporte forbiddenness of d–d transitions.[11]

The next d–d transition shown by $[AuCl_4]^-$ ions and $Au_2Cl_6(s)$ at 400–360 nm does not distinctly appear for $AlAuCl_6(g)$ and

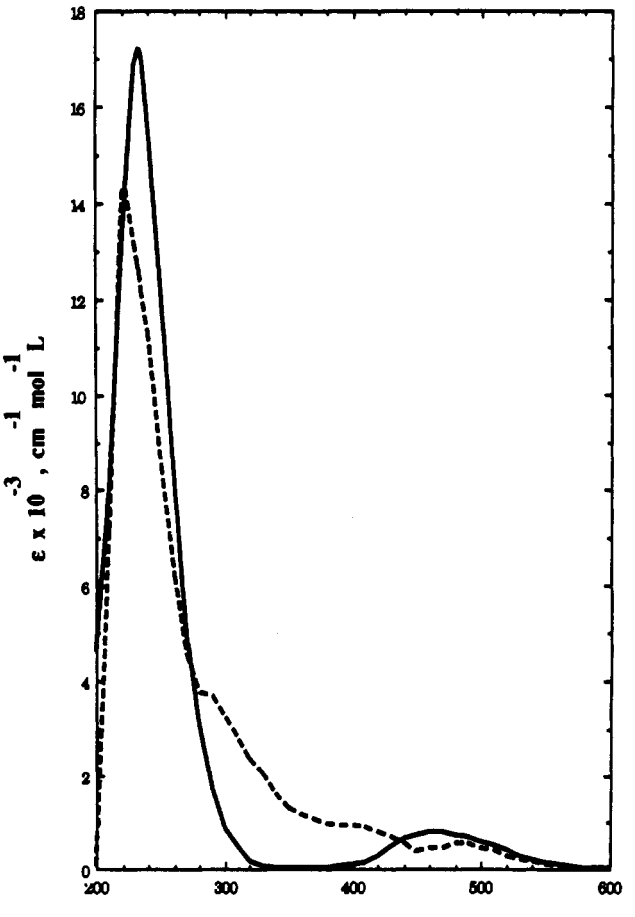

Figure 3. Derived spectra for $AlAuCl_6(g)$, solid line, and $AlAuCl_5(g)$, dashed line. Molar absorptivities are from Table III, with T = 550 K.

$Au_2Cl_6(g)$. In the gas phase these two molecules might have much more distortion than expected for Au_2Cl_6 in the solid phase, causing the ordering of the d-orbitals to change to $b_{1g} > b_{2g} > a_{1g} > e_g$. Thus, this transition for these two molecules involve two

(14) Mason, W. R.; Gray, H. B. *Inorg. Chem.* **1968**, *7*, 55.
(15) Clark, W. D.; Templeton, D. H. *Acta Crystallogr.* **1958**, *11*, 284.
(16) Silukova, T. N.; Babin, P. A.; Voropaev, S. F. *Fix. Kondensiv. Sostoyaniya Veshchestva, Khabarovsk* **1978**, 14.

σ-antibonding orbitals (a_{1g} and b_{1g}) and less vibronic coupling, resulting in more Laporte forbiddenness overall and relatively low molar absorptivities.

An $AuCl_2$ or $AlCl_2$ unit attached to an edge of an $AuCl_4$ unit would be expected to cause changes in the spectral region involving ligand-metal charge transfer compared to that for the $[AuCl_4]^-$ ion. However, $Au_2Cl_6(s)$ has energies very similar to those for the $^1A_{2u}, ^1E_u(1) \leftarrow {}^1A_{2g}$ and $^1E_u(2) \leftarrow {}^1A_{1g}$ transitions for $[AuCl_4]^-$, and $AlAuCl_6(g)$ has a similar transition to that of $^1E_u(2) \leftarrow {}^1A_g$. The apparent absence of a transition for both $Au_2Cl_6(g)$ and $AlAuCl_6(g)$ similar to $^1A_{2u}, ^1E_u(1) \leftarrow {}^1A_{1g}$ for $[AuCl_4]^-$ may be due to temperature effects on molar absorptivities. The charge-transfer molar absorptivities at the λ_{max}'s decrease and the bands broaden with increase in temperature, and this transition could be simply under the intense peak. Also, experimentally, this is the region where the chlorine absorbance is large and, thus, the largest subtraction uncertainties occur.

The $AlAuCl_6(g)$ spectrum shows only one absorption maximum for the most intense peak whereas $Au_2Cl_6(g)$ has two maxima. The λ_{max} for $AlAuCl_6(g)$ appears to be an average of those for $Au_2Cl_6(g)$. The areas, per gold atom, under the peaks are roughly the same. It appears that the 244-nm peak shifts to shorter wavelengths while the 222-nm peak shifts to longer wavelengths when one of the gold atoms in $Au_2Cl_6(g)$ is replaced by an aluminum atom. One explanation for this effect is to assume that one of the transitions for $Au_2Cl_6(g)$ involves the bridging chlorine atoms (244 nm) and the other involves the terminal chlorine atoms (222 nm).[17] Replacement of one of the Au(III) atoms with the stronger polarizing Al(III) atom (based on charge density)[18] causes the 244-nm transition to shift to shorter wavelengths. The resulting decrease in electron density on the remaining Au(III) atom causes the other transition to occur at longer wavelengths. The above assignment could be reversed and Al(III) could be less polarizing (based on Au(III) being a transition metal ion)[18] resulting in the same overall effect. However, replacing an electron on the $[AuCl_4]^-$ ion with an $AlCl_2$ or $AuCl_2$ unit should cause a significant shift to shorter wavelengths, just the opposite of that observed. Another explanation involves the bending of the bridge. Theoretical calculations[19] indicate that the two sets of d-orbitals in dimeric, square-planar complexes split depending on the "hinge" angle, and thus, two different transitions are possible. In the solid phase, Au_2Cl_6 molecular units are planar, but in the gas phase, the molecules are free to bend. With $AlAuCl_6(g)$, the tetrahedrally distributed chlorine atoms attached to the aluminum atom may stereochemically decrease the amount of bending.

The $AlAuCl_5(g)$ molecule supposedly has quite a different structure than those above. However, surprisingly, the derived spectrum correlates best with that of the $[AuCl_4]^-$ ion, except for the enhancement of the molar absorptivities of the d-d transitions. Also, λ_{max} for the intense charge-transfer band has shifted to a shorter wavelength, compared to $AlAuCl_6(g)$, as expected from the lower oxidation number on the gold atom.

Thermodynamic Constants. Equilibrium constants for reactions 1, 3, and 5 were calculated from the derived concentrations (Table S1, supplementary material). Least-squares treatments of ln K vs $1/T$ gave the constants listed in Table IV along with the corresponding thermodynamic constants. The $\Delta H°$ and $\Delta S°$ values for reactions 1 and 3, from I and II, agree within the experimental uncertainty. Enthalpy of formation and standard entropy values for $AlAuCl_6(g)$ and $AlAuCl_5(g)$ were calculated using reference data from the sources cited in the table. The entropy projected for $AlAuCl_6(g)$ when II is used is 8 J K^{-1} mol^{-1} less than when I is used. The difference, $S°(AlAuCl_6(g)) - S°(AlAuCl_5(g))$, 87 J mol^{-1} K^{-1}, is somewhat larger than found for simpler pairs of molecules which differ by one chlorine atom, e.g. $S°(FeCl_3(g)) - S°(FeCl_2(g))$ = 60 J mol^{-1} 1 K^{-1}.[9]

The results derived for reaction 1 are compatible with those expected on statistical grounds. The enthalpy change is small, and the equilibrium constant is of the order of unity; e.g. at 600 K, K_1(I) is 2.4 and K_1(II) is 1.1.

Supplementary Material Available: Table S1, a detailed listing of temperatures, observed absorbances, and derived concentrations for the various samples (3 pages). Ordering information is given on any current masthead page.

(17) Mason, W. R.; Gray, H. B. *J. Am. Chem. Soc.* **1968**, *90*, 5721.
(18) Huheey, J. E. *Inorganic Chemistry, Principles of Structure and Reactivity*, 2nd ed.; Harper and Row: New York, 1978; pp 91-92.
(19) Summerville, R. H.; Hoffmann, R. *J. Am. Chem. Soc.* **1976**, *98*, 7240.
(20) Barin, I. *Thermochemical Data of Pure substances*; VCH Publishers: New York, 1989.

Contribution from the Instituto de Química-UNESP, Caixa Postal 355, 14800 Araraquara, SP-Brazil, Instituto de Física e Química-USP, Caixa Postal 369, 13560 São Carlos, SP-Brazil, and Department of Chemistry, Washington State University, Pullman, Washington 99164-4630

Synthesis, Structure, and Electronic and EPR Spectra of Copper(II) Complexes Containing the $[CuBr_4]^{2-}$ Anion and Triphenylarsine Oxide

Antonio Carlos Massabni,† Otaciro Rangel Nascimento,‡ Kristopher Halvorson,§ and Roger D. Willett*,§

Received June 11, 1991

The preparation and characterization of $(Ph_3AsOH)_2[CuBr_4]$ and $[Cu(Ph_3AsO)_4][CuBr_4]$ are reported (Ph_3AsO = triphenylarsine oxide). Crystallographic analysis of the monoclinic crystals of $(Ph_3AsOH)_2[CuBr_4]$ (space group $C2/c$, a = 17.569 (3) Å, b = 13.090 (2) Å, c = 16.933 (2) Å, and β = 105.64 (2)°, R = 0.055 and R_w = 0.057) revealed the presence of compressed $[CuBr_4]^{2-}$ tetrahedra of C_2 symmetry with Cu-Br distances of 2.340 (1) and 2.437 (1) Å and *trans*-Br-Cu-Br angles of 139.2 (1) and 122.4 (1)°. The oxonium cations hydrogen bond to the bromine atoms involved in the longer Cu-Br bonds and the smaller *trans*-Br-Cu-Br angle. Single-crystal electronic and EPR spectra are interpreted in terms of the observed $[CuBr_4]^{2-}$ geometry. Analysis of the electronic and EPR spectra of $[Cu(Ph_3AsO)_4][CuBr_4]$ led to the postulation of the presence of planar $[Cu(Ph_3AsO)_4]^{2+}$ cations and distorted tetrahedral $[CuBr_4]^{2-}$ anions.

Introduction

Copper(II) complexes with phosphine and arsine oxides, mainly Ph_3AsO, have been obtained and studied in one of our laboratories. Square-planar complexes containing the cation $[Cu(Ph_3AsO)_4]^{2+}$ and the anions ClO_4^-, NO_3^-, and $[Cu^ICl_2]^-$ were previously described.[1] Compounds with the anion $[CuX_4]^{2-}$ (X = Cl^-, Br^-) were also studied.[2] In the presence of strong acid, protonation

† Instituto de Química-UNESP.
‡ Instituto de Física e Química-USP.
§ Washington State University.

(1) Nascimento, O. R.; Massabni, A. C. *Polyhedron* **1985**, *4*, 707.
(2) (a) Massabni, A. C.; Nascimento, O. R.; Almeida Santos, R. H.; Francisco, R. H. P.; Lechat, J. R. *Inorg. Chim. Acta* **1983**, *72*, 127. (b) Halvorson, K. E.; Willett, R. D.; Massabni, A. C. *J. Chem. Soc., Chem. Commun.* **1990**, 346.

0020-1669/92/1331-1779$03.00/0